Electronic Supplementary Material (ESI) for Soft Matter.

Supplementary Information

Patterning of perovskite-polymer films by wrinkling instabilities

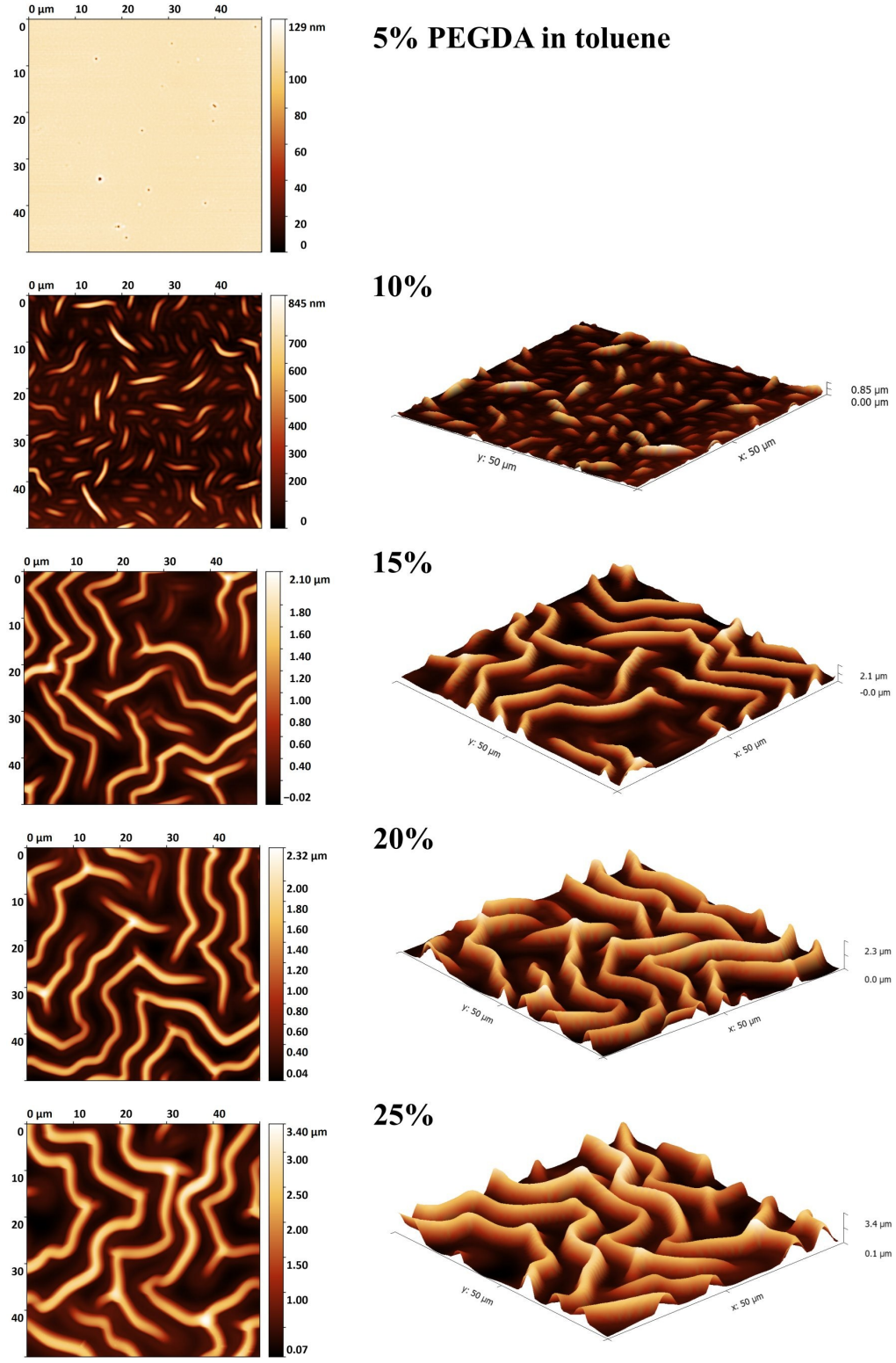

Figure S1 Atomic force microscopy (AFM) images of wrinkled PEGDA films after exposure to O_2 plasma. Films were prepared by spin-coating solutions of different PEGDA concentrations in toluene (5% to 25% (v/v)) atop FTO-coated glass at a constant spin-coating speed of 8000 rpm. The resulting films had a different initial thickness (c.f. Figure S2). It is evident that both the height and the width of the wrinkles increased with increasing PEGDA concentration (film thickness, c.f. Figure S2). While no wrinkles were observed for the lowest concentration (5%), the average height of the wrinkles was found to increase from 0.3 µm to 1.7 µm when increasing the polymer concentration from 10% to 25%.

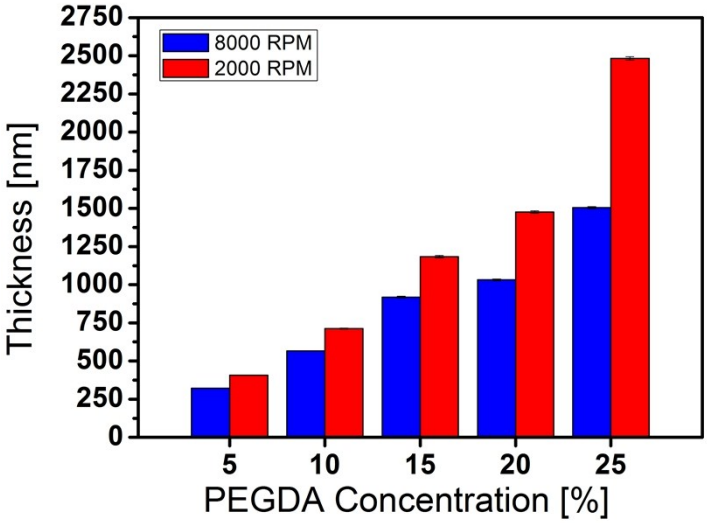

Figure S2 Thickness of PEGDA films as measured by means of ellipsometry as a function of the polymer concentration in toluene for two different spin-coating speeds. Changing both, the PEGDA concentration in toluene as well as spin-coating speed allowed for varying the thickness of PEGDA films between around 280 nm and about 2500 nm.

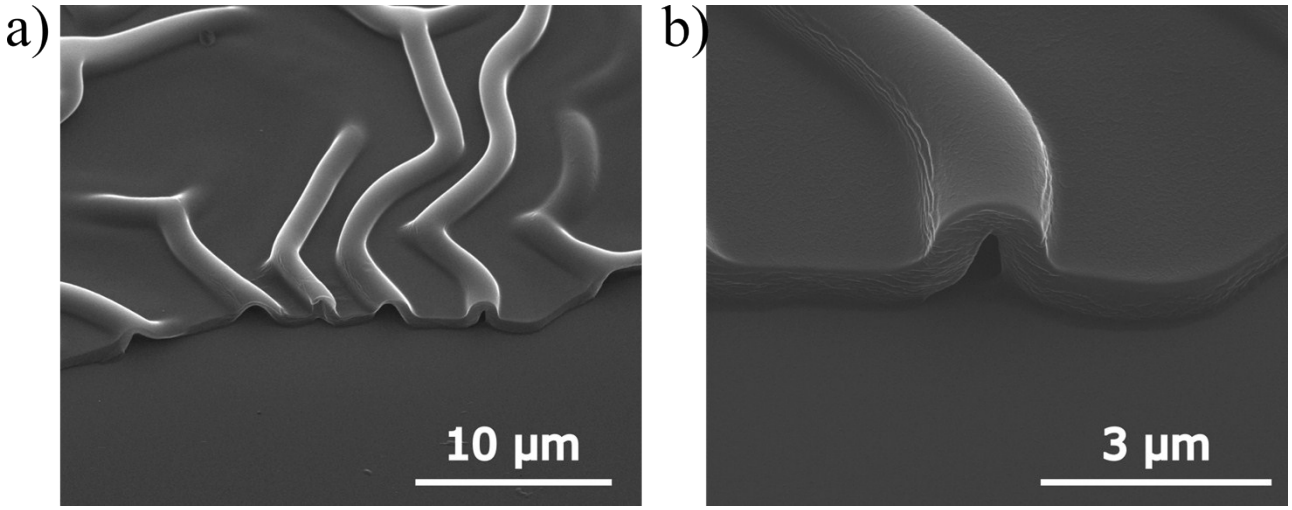

Figure S3 SEM image of a wrinkled PEGDA film (20 vol% PEGDA/toluene, spin coated at 6000 rpm) showing the thickness of the polymer layer and the shape of the wrinkles.

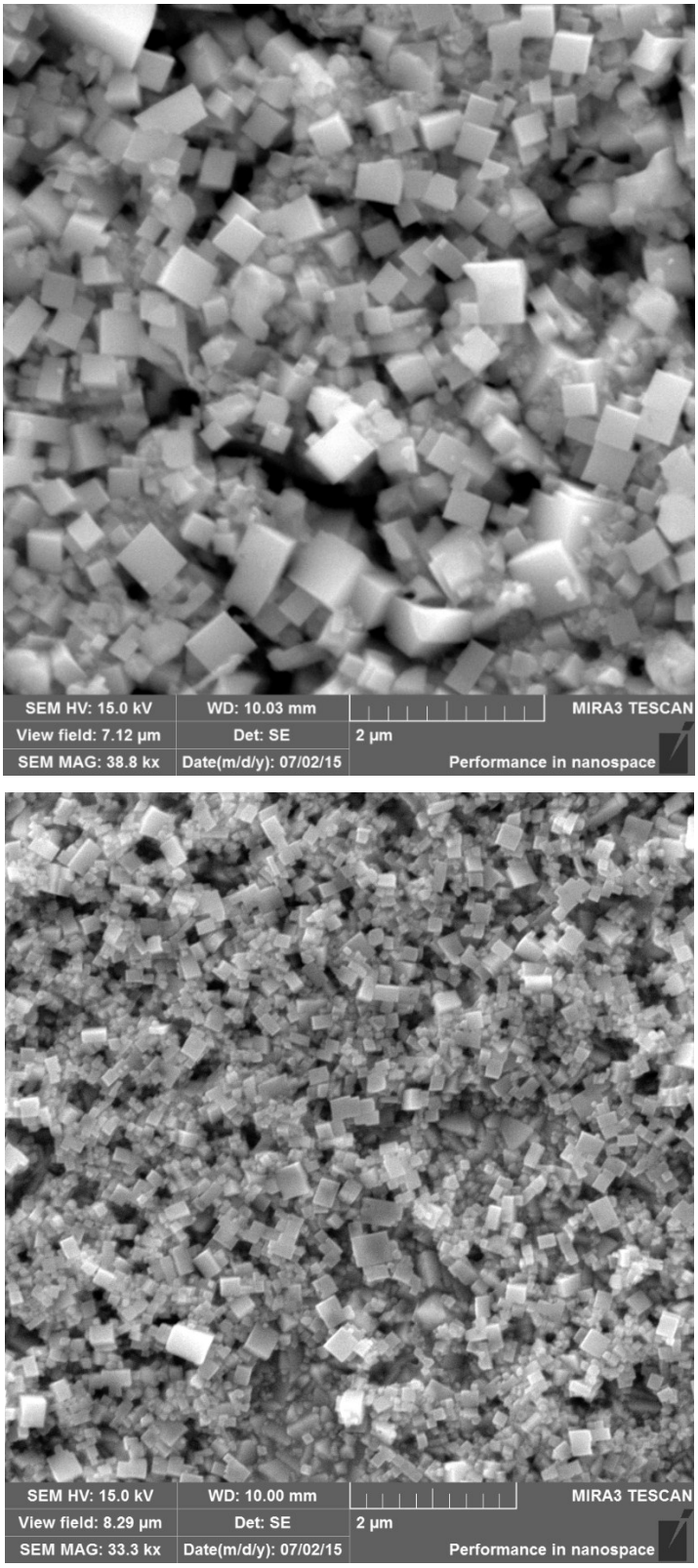

Figure S4 SEM images of perovskite nanocrystals synthesized from a 0.5 M (top) and 0.01 M (bottom) precursor solution.

Dynamic Light Scattering

Standard dynamic light scattering (DLS) data were collected at constant temperature (21 °C) at 90 deg., using a commercial goniometer instrument (3D LS Spectrometer, LS Instruments AG, Switzerland). The primary beam was formed by a linearly polarized and collimated laser beam (Cobolt 05-01 diode pumped solid state laser, λ = 660 nm, P_{max} = 500 mW), and the scattered light was collected by single-mode optical fibers equipped with integrated collimation optics. The collected light was coupled into two high-sensitivity APD detectors via laser-line filters (Perkin Elmer, Single Photon Counting Module), and their outputs were fed into a two-channel multiple-tau correlator. The signal-to-noise ratio was improved by cross-correlating these two channels. The corresponding field auto-correlation functions were obtained via the Siegert relation: $g_1(t) = \sqrt{g_2(t) - 1}$ where $g_2(t)$ is the intensity auto-correlation function constructed from the temporal fluctuations of the depolarized component of the scattered intensity.

For a dilute suspension of uniform spherical NPs of radius r, the correlation function is written as,

Equation 1 $$g_1(t) = e^{-\Gamma(q,r)t}$$

where

Equation 2 $$\Gamma(q,r) \equiv q^2 D_T$$

and

Equation 3 $$D_T = \frac{k_B T}{6 \pi \eta} \frac{1}{r}$$

k_B is the Boltzmann constant, T the temperature, η the viscosity of the solvent, q the momentum transfer $q = \frac{4\pi}{\lambda} n \sin\left(\frac{\theta}{2}\right)$, θ the scattering angle, λ the wavelength of the scattered waves, and n the refractive index of the solvent.

The field correlation function from polydisperse samples is frequently expressed as the Laplace transform of the probability density function describing the dispersion in the relaxation rate. Then the correlation function (Equation 1) is written as

$$g_1(t) = \int_0^\infty P(\Gamma)\, e^{-\Gamma t}\, d\Gamma$$

Equation 4

where $P(\Gamma)$ is the probability density function of the relaxation rates. $P_\Gamma(\Gamma)$ is modelled here by the (modified) Schulz–Zimm distribution:

$$P(\Gamma) = \frac{1}{\Gamma\left(\frac{1}{\sigma^2}\right)} e^{-\frac{\Gamma}{\langle\Gamma\rangle\,\sigma^2}} \left(\frac{1}{\langle\Gamma\rangle\,\sigma^2}\right)^{\frac{1}{\sigma^2}} \Gamma^{\frac{1}{\sigma^2}-1}$$

Equation 5

where

$$\langle\Gamma\rangle \equiv \int_0^\infty \Gamma P(\Gamma) d\Gamma$$

Equation 6

and

$$\sigma(\Gamma) \equiv \frac{\sqrt{var\Gamma}}{\langle\Gamma\rangle}$$

Equation 7

In case of a unimodal distribution $0 < \sigma \leq 1$. When σ is close to 1, the Schulz–Zimm distribution approaches an exponential distribution, and when σ is small, it approaches a Gaussian distribution. According to Equation 5, the correlation function is now written as

$$g_1(t) = \left(1 + \langle\Gamma\rangle\sigma^2 t\right)^{-\frac{1}{\sigma^2}}.$$

Equation 8

The correlation functions and their respective best fit (Figure S1, Equation 8) corresponding to the three different concentrations of the perovskite precursor solution are shown below. The estimated apparent intensity-weighted average hydrodynamic radii were 807 nm, 338 nm and 129 nm for 0.5M, 0.1M and 0.01M solutions, respectively. The intensity-weighted probability function of the hydrodynamic radius, $P_r(r)$, is estimated via applying the rule of transforming random variables. Let Φ represent the relationship between Γ and r (Equation 2 and 3). Then the probability density function of the intensity-weighted hydrodynamic radius is estimated via

$$P_r(r) = P_\Gamma(\Phi(r)) \cdot \left|\frac{d}{dr}\Phi(r)\right|$$

Equation 9

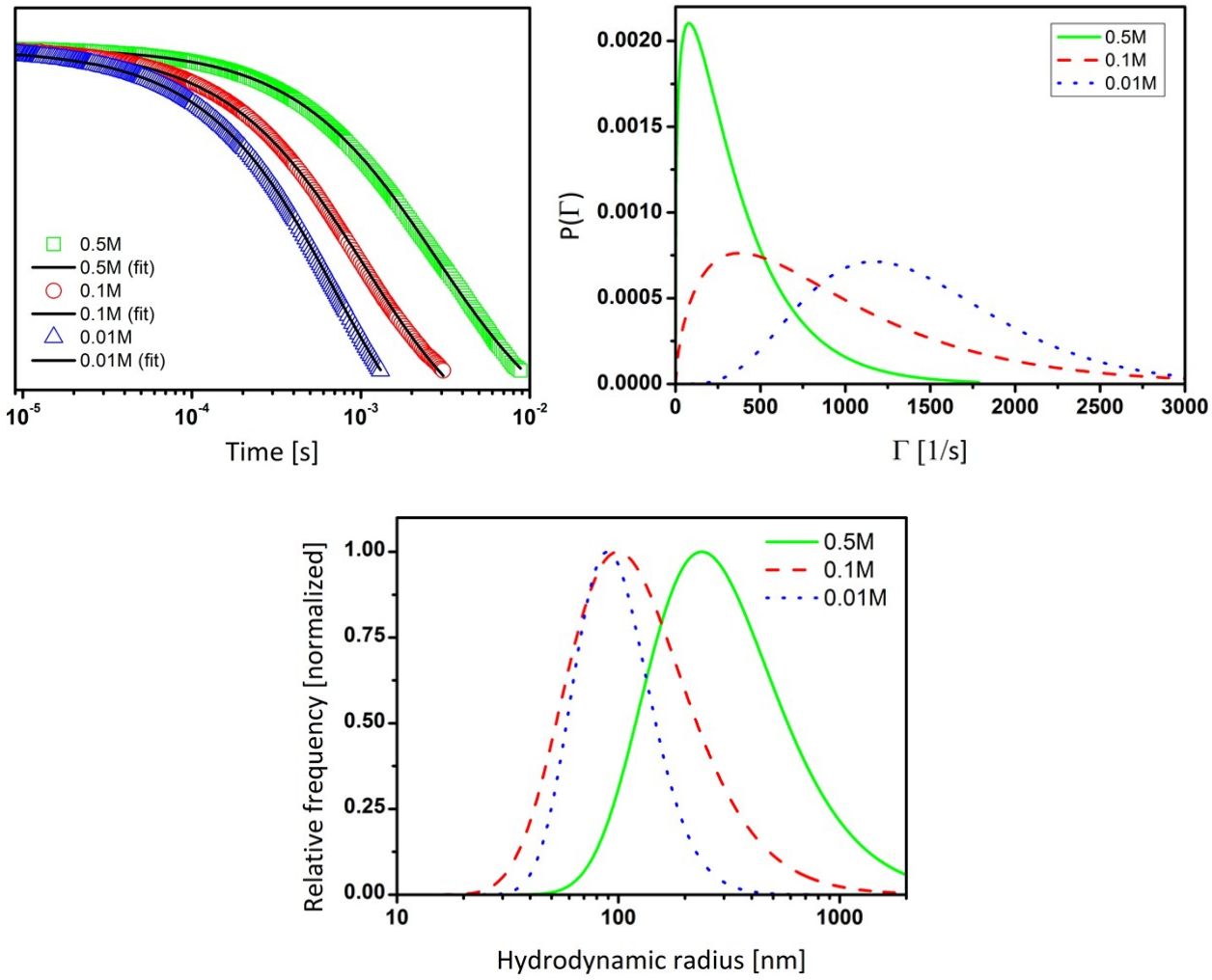

Figure S5 Correlation function and model fit (left) of the Equation 8 for 0.5M, 0.1M and 0.01M precursor solution concentrations (top left). Probability density function of the relaxation rates for the three samples (top right). Intensity-weighted probability density function of the hydrodynamic radius (bottom).

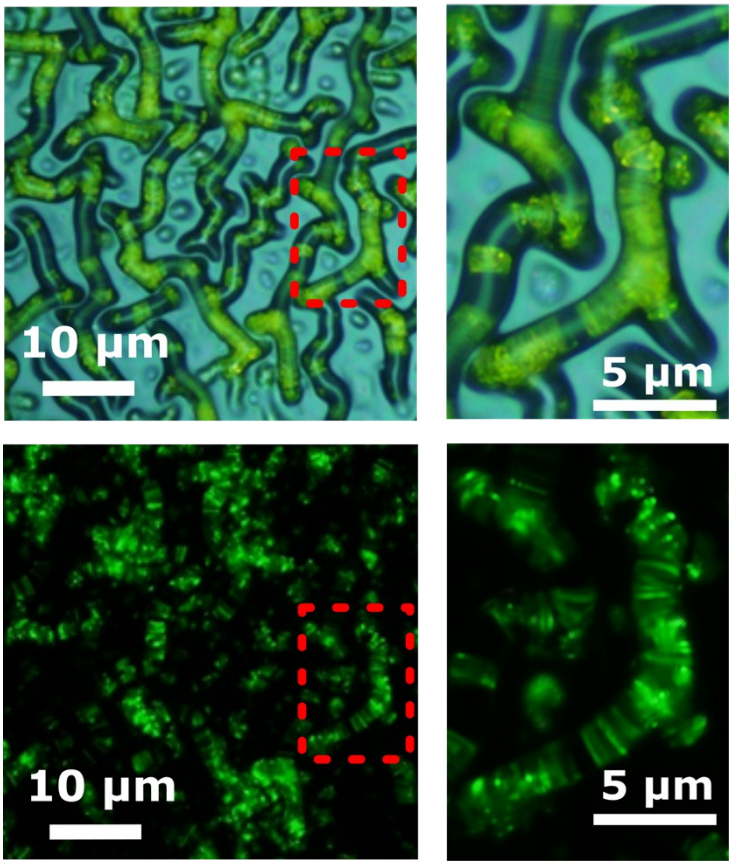

Figure S6 Preferential localization of perovskite crystals inside the ridges of a wrinkle pattern as shown by means of visible light microscopy (top) and under UV illumination (bottom). The green fluorescence emission of perovskite nanocrystals can be observed under UV light. Magnified images are shown on the right.

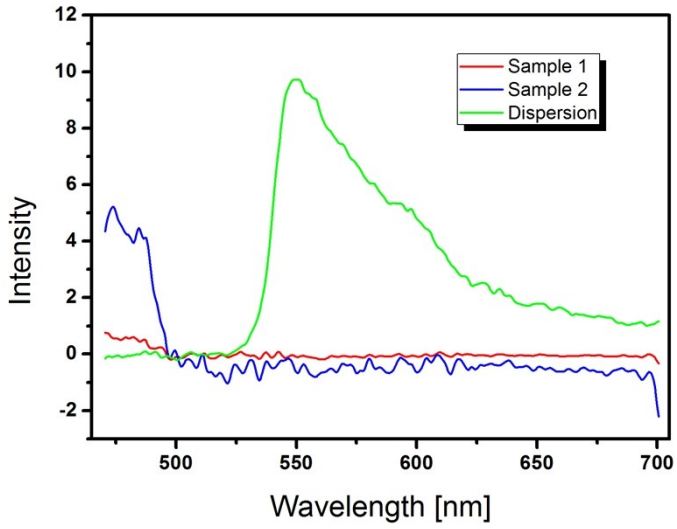

Figure S7 Photoluminescence spectra collected using an integrating sphere of a film with (Sample 1) and without the perovskite crystals (Sample 2) and toluene dispersion of perovskite crystals. The signal from the film is too weak to quantify the emissive efficiency. This is due to the fact that the smallest particle size obtained with the method in this work (100 nm) is too large to get a high enough dispersion of particles in solution and thus in the film.

Cerda and Mahadevan derived the following equations for the wavelength λ and amplitude *A* of wrinkles on a thin sheet of length *L*, width *W*, thickness *t*, elastic modulus *B*, imposed transverse displacement Δ, and tension *T*:

$$\lambda = 2\sqrt{\pi}\left(\frac{B}{T}\right)^{\frac{1}{4}} L^{\frac{1}{2}}$$

$$A = \frac{\sqrt{2}}{\pi}\left(\frac{\Delta}{W}\right)^{\frac{1}{2}} \lambda$$

For a stretched sheet these equation become:

$$\lambda = \frac{(2\pi L t)^{\frac{1}{2}}}{\left[3(1-\nu^2)\gamma\right]^{\frac{1}{4}}}$$

$$A = (\nu L t)^{\frac{1}{2}}\left[\frac{16\gamma}{3\pi^2(1-\nu^2)}\right]^{\frac{1}{4}}$$

So the amplitude of the wrinkles is dependent upon the thickness of the film with a power law dependence with exponent 0.5. So, using the basic properties of logarithms:

$$\log(A) \propto 0.5 \log(t) + C$$

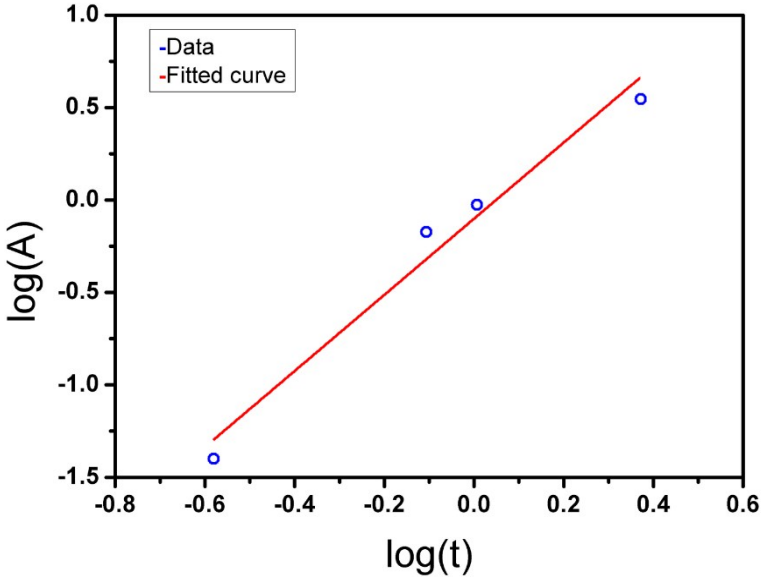

Figure S8. Linear best fit of the wrinkle amplitude as function of initial PEGDA film thickness (red line is a fit to: log(A)=a*log(t)+b; with a = 2.013; b = -0.1543).

Figure S7 reports the linear best fit of the logarithm of the wrinkle height as a function of the initial film thickness. Although the general behaviour is in agreement with the Cerda and Mahadevan theory (i.e. it is possible to increase the amplitude of the wrinkles by increasing the thickness of the film) the angular coefficient of the fitting line is ~2, far from the expected 0.5. This is probably due to the very simple model used, which approximates the PEGDA to a homogeneous film subjected to a compressive internal stress. In our case, the PEGDA film most probably has a longitudinal anisotropy with the elastic modulus varying throughout the thickness of the material, due to the different plasma exposure leading to a gradient in the crosslinking degree along the vertical direction (see Chandra et al, "Self-Wrinkling of UV-Cured Polymer Films", , *Advanced Materials*, 23(30), pp.3441-3445). We can approximate this system with a two-layer film

with a constant “hard skin” of thickness h_s and a varying “soft skin” of thickness h. So the total thickness will be $t=h_s+h$. In this approximation we can use the relationship found by Cerda and Mahadevan:

$$A \propto \lambda \propto (hh_s)^{\frac{1}{2}} \rightarrow \log(A) \propto 0.5 log(t - h_s)$$

because $h_s = h_s(t - h_s)$ and, using the properties of logarithms, $\log(h_s(t - h_s)) = \log(t - h_s) + const.$

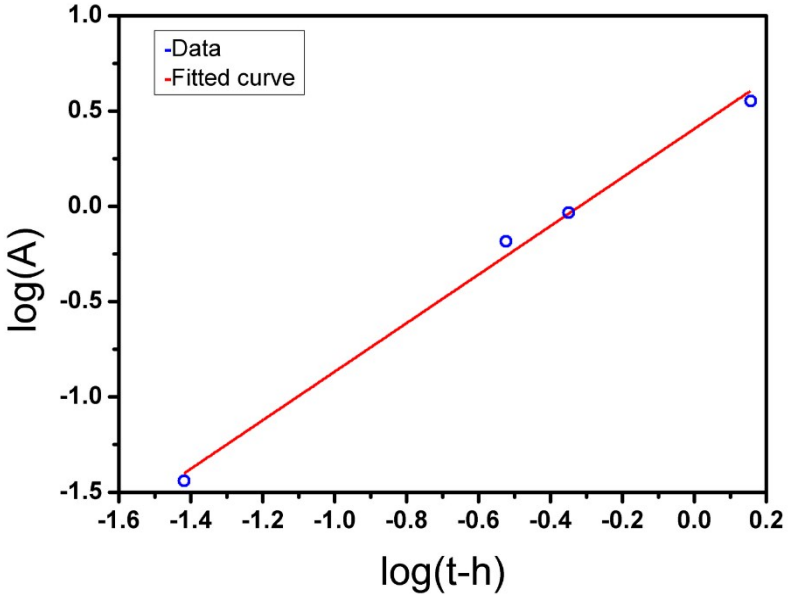

Figure S9. Linear best fit of wrinkles amplitude as function of initial PEGDA film thickness using the two-layer approximation (red line is fit to log(A)=a*log(t-h)+b; with h = 0.322; a = 1.246; b = 0.3921).

In Figure S9 the linear best fit of *log(A)* as function of *log(t-h_s)* is shown. The hard skin thickness has been chosen to be equal to 0.322 because for this thickness no wrinkles are formed (c.f. with Figs. 1d and S1). As we can see the angular coefficient of the fitting line is ~1.2, which is significantly closer to the angular coefficient of 0.5 predicted from the Cerda and Mahadevan model than the value we obtained with a simple homogeneous film approximation. This confirms our hypothesis that the anisotropy with the elastic modulus varying through the thickness makes our system more complex than a single or double layer film approximation of the Cerda and Mahadevan model.